Title: When record breaking heat waves should not surprise: skewness, heavy tails and implications for risk assessment

Authors: N. Bjarke[1]*, J. J. Barsugli[2], M. P. Hoerling[2], X.-W. Quan[2], B. Livneh[1,3]

Affiliations:

[1]Department of Civil, Environmental, and Architectural Engineering, University of Colorado, Boulder; Boulder, Colorado 80309, United States of America.

[2]Natonal Oceanic and Atmospheric Administration, Physical Sciences Laboratory; Boulder, Colorado 80305-3328, United States of America.

[3]Cooperative Institute for Research in Environmental Sciences; Boulder, Colorado 80309, United States of America.

*Corresponding author. Email: Nels.Bjarke@colorado.edu

Abstract: Extreme heat waves beset western North America during 2021, including a 46.7°C (116°F) observation in Portland, Oregon, an astonishing 5°C above the previous record. Using Portland as an example we provide evidence for a latent risk of extreme heat waves in the Pacific Northwest (PNW) and along the west coast of the United States where a maritime climate and its intrinsic variations yield a positive skewness in summertime daily maximum temperatures. A generalized Pareto extreme value analysis yields a heavy tailed distribution with a return period of 300-1000 years, indicating that, while rare, the event was possible, contrary to prior claims that the event was "virtually impossible". We demonstrate that the extreme temperatures can be explained by the coincident extreme values of geopotential heights, and that the relationship between heights and extreme temperatures has not materially changed over the observational record. The dynamical nature of the event along with recent developments in stochastic theory justifies the use of skewed and heavy-tailed distributions which may provide the basis for a more proactive approach to managing the risk of future events.

Key Words: Heat wave**,** probability, climate change, risk

1. Introduction

The 2021, early-summer heat wave in the Pacific Northwest (PNW) of the United States and southwest British Columbia, Canada, broke numerous all-time records for daily maximum temperature (T_{max}), resulting in hundreds of hospitalizations and deaths in the region (*1*). The heat wave was notable in that many records were not only broken, but were far exceeded (*2*, *3*), including a record in Portland Oregon of 46.7°C (116°F) on the 28 June (Figure 1) that was 5°C (9° F) higher than the previous record for any day and 7.8°C (14°F) higher than the previous record for any day in June (*4*). National Weather Service forecasts for the Portland region warned of record-breaking temperatures and an "unprecedented heat wave" (*5*) for several days

preceding the event, with the event's expectation itself generating significant media coverage (*1*, *2*, *6*). Some numerical weather prediction models had been forecasting greater than 43.3°C (110°F) temperatures for over a week prior to the event.

Such warnings notwithstanding, the event was surprising from a climatological perspective for this typically maritime dominated climate west of the Cascade mountains. The event severely tested resilience and in some cases exposed unforeseen vulnerabilities. In particular, the health impacts of this heat wave may have been exacerbated given acclimation to cooler conditions and by the surprising extremity of the temperature. In addition, prior assessments of observed trends and anthropogenic climate change focused on the greater potential for increases in the severity of nighttime (T_{min}), rather than daytime (T_{max}) heat waves in the coastal regions of the western US (*7–10*), or that heat waves would be moderated in coastal regions of the PNW (*11*) giving less reason to expect—and perhaps mitigate the effect of—such an extreme daytime heat event in 2021.

The severity of the PNW heat wave and its impacts on human health motivated investigations into its return period. Given knowledge of historical variability together with the fact that anthropogenic forcing is increasing global temperatures, the question arises how probable such an event is in today's climate (*3*). One such estimate deemed the 2021 PNW heat wave 'virtually impossible', with greater than 150,000 year return period, even including an estimate of the trends in extreme values due to the influence of climate change. A moderated estimate of a 1,000 year return period, still pointing to extremely unlikely occurrence, was reached when including the event in the statistical fit (a procedure which does not allow one to foresee such an event). The interpretation from these initial analyses is that the event was nearly impossible to foresee even when accounting for present-day climate change drivers (*3*). These are not entirely satisfying conclusions given the certainty and occurrence of the event in 2021. In particular, the following questions remain unanswered: *1) Why was the PNW heat-wave so extreme relative to extreme heat events across the rest of the western US that summer?*, *2) Could an alternative statistical analysis of the historical record have better forewarned of the possibility for an event like the 2021 PNW heat wave?, and 3) Is the PNW, among other possible areas, susceptible to such "surprises" owing to inherent physical constraints operating on their local historical temperature variability?* Here we consider each of these questions.

2. Materials and Methods

This analysis relies on historical climatological observations of temperature and geopotential heights for the Portland, OR International Airport station (KPDX) for the years leading up to the 2021 PNW heat wave and the event itself (Sec. 2.1). We apply both Generalized Extreme Value (Sec. 2.2) and Generalized Pareto Distribution (Sec 2.3) methodologies to estimate the probability of the 2021 event and utilize bootstrapping to quantify uncertainty in those estimations (Sec. 2.4). Following this, we leverage a Stochastically Generated Skew analysis based on recent advances in stochastic theory (Sec. 2.5) to support the results from the estimation of the event probability and then produce a regression analysis relating temperature extremes to geopotential heights (Sec. 2.6) to further support our understanding of the potential for the 2021 event.

2.1 Climate Observations

Observations of daily maximum temperature (T_{max}) were taken from the Global Historical Climatology Network daily (GHCNd) dataset of station climate observations (*4,17*) across North America. . Climate stations were screened to ensure sufficient record length for statistical evaluation. Station screening criteria required at least 50 years of data as of June 2020 and a minimum of 90% of valid daily observations of T_{max} during the months of May-August, i.e., non-missing data that pass quality control flagging applied by GHCNd (*4*, *17*). The latitude and longitude information provided by GHCNd was used to map the location of all stations.

The daily 500 hPa geopotential height index (GHI) was calculated as the area average geopotential height over the latitude-longitude rectangle bounded by 47°N-57°N, 135°W-120°W. This area is the center of action for the composite of 500 hPa height anomalies associated with Pacific Northwest daytime (T_{max}) heatwaves as demonstrated in Figure 3 of Bumbaco et al. (2013). Heights were obtained from the NCEP/NCAR reanalysis for the period 1948-2021. Only data between 15 June and 15 July of each year were subsequently used in the analysis. This date range was selected so that the observations are centered on the date of occurrence of the 2021 Pacific Northwest heatwave and to partially mitigate the influence of a seasonal temperature cycle on the estimation of the probability of extremes. The sample skewness of daily T_{max} was calculated from June 15th to July 15th for each station, shown in Fig. 2, across all years on record using the Fisher-Pearson coefficient of skewness (*18*).

2.2 Generalized Extreme Value Analysis

Estimation of the Generalized Extreme Value (GEV) distribution for Portland T_{max} utilizes the annual maxima for each year over the period 1948-2020, resulting in a sample size of n=73. Scale, location, and shape parameters for the GEV distribution were estimated from the data using the Maximum Likelihood Estimator (MLE) method described in (*19*) and executed using tools in the Python SciPy library (*20*). Estimated parameters were then used to generate a probability density function (PDF) of the GEV distribution from which we could calculate the probability of a 46.7 °C T_{max} event. Our analysis adopted the convention that a negative shape parameter corresponds with a Weibull form of GEV and a positive shape parameter corresponds to a Fréchet form of GEV. We show in Fig. 3 that estimated parameters from the annual block-maxima record of T_{max} for Portland produce a GEV PDF that returns a zero probability of a 46.7 °C T_{max} event. Inset panels that show the uncertainty of the estimated return period equivalent to those shown for the Generalized Pareto Distribution were not included for GEV as the observations produce no parameter estimates that allow for the estimation of non-zero probabilities for the T_{max} magnitude observed in Portland during the 2021 heatwave, consistent with a Weibull type GEV.

2.3. Generalized Pareto Distribution Analysis

The Generalized Pareto Distribution (GPD) was applied to estimate the probability distribution of peaks over a threshold. We computed GPD estimates based on thresholds of the 90th and 95th percentiles from all observed daily records of T_{max} from June 15th to July 15th across all years. The GPD parameters (shape, scale and location) were estimated using methods outlined in (*21*, *22*). The parameters were applied to generate a probability density function

(PDF) using tools in the Python SciPy library (*20*). The PDF was then used to estimate the exceedance probability of a daily T_{max} of 46.7 °C, which was converted to a return period using methods described in (*23*, *24*).

2.4. Uncertainty in GEV and GPD parameters

Uncertainty bounds for the return period calculation were estimated (*21*) using bootstrap resampling with replacement. For the GEV analysis, years were resampled with replacement to create 10,000 bootstrap samples from which GEV parameters were calculated. For the GPD analysis daily T_{max} values within the seasonal window of June 15th – July 15th were resampled with replacement to create 10,000 samples of the equivalent size to the historical daily T_{max} (n=2,263 days). GEV resampling yielded no samples with a finite return period for the Portland record event. The histogram of bootstrap generated GPD return periods is shown in the inset panels of Fig 3. The estimated return period uncertainty bounds reported in the manuscript represent the 2.5 and 97.5 percentile values from the distribution of ranked estimated return periods. Reported for both 90th and 95th percentile thresholds, the central GPD fits are the median values of annual return period from all 10,000 boot-strapped samples.

2.5. Stochastically Generated Skew (SGS) Analysis

The Stochastically Generated Skew (SGS) distribution estimates were made using the online ATMOS Distributions tool from Web-based Reanalyses Intercomparison Tools (WRIT, https://psl.noaa.gov/data/writ/) including the option to analyze station data from the GHCN dataset. As only whole months are available as options we chose to include data from the months of June and July, for the 1948-2016 time period. At the time of this analysis, only data through 2016 were available in that web tool. In calculating the return period, we computed the autocorrelation of T_{max} to estimate the number of effective samples in the June-July period. See for example, (*25*) for a discussion of autocorrelation in T_{max}, and (*26*) for the role of autocorrelation in the stochastic process that generates the SGS distribution.

2.6. Regression Analysis

We fit a linear regression predictive model on the 500 hPa geopotential height index to predict T_{max} for all daily observations for both the early (1948-1983) and late (1984-2020) periods using methods described in (*27*) and tools from the Python SciPy library (*20*). The best fit linear regression using a least-squares method is plotted on Fig. 4 as a solid green/orange line. The period of record was split into two periods of equal length—mid-20th century (1948-1984), and late-20th-to-early-21st century (1984-2020)—in order to evaluate potential climatological changes in the linear relationship between 500 hPa geopotential height anomalies and T_{max}.

In order to estimate the dependence of probable extremes on geopotential heights from the historical record we applied a linear regression predictive model to the 99th percentile of T_{max} observations from uniformly binned sub-samples of the coinciding observations of 500 hPa geopotential heights. All observations of 500 hPa heights were sorted in ascending order and sub-sampled into bins of 100 observations each. For each bin, we selected the observation pair of 500 hPa geopotential height and T_{max} with the greatest magnitude of T_{max}, approximating the 99th

percentile for this bin. This process was repeated until the entire sample of daily June 15th to July 15th observations from 1948-2020 was analyzed. The same linear regression predictive model technique described above was then applied to the 99th percentile sub-set of observations with the best fit linear regression shown on Fig. 4 as a solid black line.

For each regression line, we also plot a shaded region of the like color for the corresponding best fit model that represents the in-sample boot-strapped 95% confidence interval of the linear regression using methods described in (*28*) and executed using tools from the Python Seaborn library (*29*). The 95% out of sample confidence interval, often called the prediction interval, was estimated for the quantile regression using methods described in (*30*) and the upper and lower bounds of that interval are shown as dotted black lines.

3. Results and Discussion

Why was the PNW heatwave so extreme compared to extreme heat events across the rest of the western US that summer? Estimation of the probability of events of record-breaking magnitude presents a major challenge as it is necessarily an extrapolation from observed data. Uncertainties due to choice of statistical method/model, short length of the observed record, and climate non-stationarity can lead to inaccurate estimation of the likelihood of a record-breaking extreme event (*12–15*). Furthermore, infrequent, heat wave-inducing atmospheric circulation patterns can produce extreme heat events that fall far outside the range of observed maximum temperatures (*16*). Though these challenges are ever present for planning and risk management, historical meteorological observations can help to identify regions at higher risk of record-breaking temperatures. Here, by taking Portland, OR as an example, we demonstrate how positively skewed regions, i.e., those with a longer tail of the daily temperature distribution for hot values, such as the PNW have a higher potential for record-breaking heat waves than other regions across the interior western US.

Daily T_{max} observations from the Global Historical Climate Network (GHCN) stations reveal a positive skewness in early-summer (June 15th – July 15th) for the PNW and along the entire West Coast (Figure 2). The long right (hot) tail of the empirical probability density function (PDF) associated with positive skewness indicates the potential for larger temperature excursions–greater hot deviations from normal–compared to the interior southwest US where the skewness is negative and the right (hot) tail of the PDF is actually shortened. (Figure 2). Positively skewed T_{max} have been widely observed in coastal regions (*31*). These are attributed to the infrequent advection of inland hot air masses that briefly replace the more typical maritime airmass that moderate temperatures via sea breezes that spread the influence of cool ocean temperatures (*31*) and associated low clouds onto the coastal margin (*32*). In the farther inland PNW (~100 km from the coast, in the Puget Sound trough and the Willamette Valley), the long positive tail of the historical T_{max} PDF has been associated with both a failure of maritime temperature modulation paired with downslope warming along the western slope of the Cascades (*10*). This historic PNW heat wave exemplified each of these operative but rare conditions in the days leading up to and during the 26th-28th of June 2021.

Could an alternative statistical analysis of the historical record have better forewarned of the possibility for an event akin to the 2021 PNW heat wave? Because daily T_{max} at the local and regional scale is non-Gaussian across much of North America (*16*, *31*, *33*), statistical methods must take such non-Gaussianity (*14*, *26*, *34*) into account to ensure robust estimation of the likelihood for extreme temperature events. Here we apply two parametric statistical methods from extreme value theory and describe how the choice of methodology could limit the ability to anticipate a record-breaking heat wave, leading to unwarranted surprise when such an event arises.

The generalized extreme value (GEV) distribution is a three-parameter (location, scale, and shape) distribution used to model the distribution of block-maxima of a random process, in this case to seasonal or annual meteorological extremes (*3*, *35–37*). The sign of the shape parameter is critical in determining the qualitative nature of extremes. Estimations of the shape parameter of the GEV distribution for maximum annual temperatures often yield a negative value (*3*), which implies a strict upper bound on the maximum possible temperature that can arise from the upper tail distribution (*15*). The implication is that the rarity of a single event above that bound is, from a frequentist perspective, thought to be not significantly distinguishable from zero probability (*14*). Because of the difficulty in estimating the shape parameter the value is sometimes determined from a regional analysis or by assuming a "typical" value. The analysis in (*3*) assumes the shape parameter is -0.2 for the Southwest US overall.

The Generalized Pareto Distribution (GPD), another commonly applied three-parameter distribution, is used to directly model the tail distribution by looking only at peak values over a given threshold. This approach has the feature of more flexibly capturing the extreme behavior of a distribution (*22*, *38*), although it is sensitive to the threshold that is set for the peaks (*39*). Lower thresholds allow for larger samples at the expense of introducing some bias into the estimates. Here we use GPD to demonstrate how such an alternate, but justifiable, method to GEV could inform estimates of heat wave probability and answer the question of why the PNW heat wave was so extreme compared to concurrent extreme heat events across the rest of the western US in 2021 (Figure 3), and importantly why the event should not have surprised.

The GEV fit to the Portland annual maximum T_{max} data indicates a negative shape parameter and zero probability (infinite return period) of the June 28, 2021 event. On the other hand, the GPD fit yields a positive shape parameter corresponding to a heavy upper tail and finite return periods. For peaks over the 90th percentile threshold the estimated return period is 337 years, 95% CI [62, 687], and for peaks over the 95th percentile the return period is 1,188 years, 95% CI [152, 2248]. The uncertainty in the mean return period stemming from different but reasonable choices of the threshold is ~ 200 years (Figure 3). Even taking this range of estimated return periods into account as some indication of uncertainty, the contrast to the GEV estimate is evident with results from the latter all but indicating the 2021 heat wave event could not have occurred, echoing the conclusions of (*3*). Critically, we can see the problematic nature of GEV for the analysis of Portland data due to its estimated negative shape parameter and hence strict upper bound on the potential maximum daily temperatures beyond which all events are considered to have zero probability (Figure 3). Such an event did in fact occur. That GPD estimates a non-negligible probability of the event using only prior data offers an obvious strength compared to GEV from a risk-management perspective.

While in theory GEV and GPD analyses should return the same shape parameter, the use of these distributions is strictly justified only in an asymptotic sense: large block size from which the maximum is selected for GEV, and high threshold above which peaks are chosen for GPD. The limitations of real-world temperature data imply that these functional forms and parametric fits will only be approximate. The GEV block size is inherently limited by the choice of summer months when annual maxima occur, whereas the GPD threshold is limited by the sample size, which in turn is only limited by the period of record. One might conjecture that for annual maximum temperature where long records are available, GPD may be a more robust method, however more research would be needed to establish this. Instead, we discuss below a third approach using stochastic theory, that suggests a heavy tailed GPD may be the appropriate functional form for regions of skewed temperature distribution.

Is the PNW, among other possible areas, susceptible to such "surprises" owing to inherent physical constraints operating on their local temperature variations? Regional heat waves in the PNW have been historically linked to ridges in the 500 hPa heights of the atmosphere (*10*), so we examine the potential for the 2021 event from a dynamical perspective based on assessing atmospheric circulation conditions that accompanied the "heat-dome" of late June 2021 (*6*). We calculated a 500 hPa geopotential height index (GHI) based on the composite 500 hPa pattern associated with daytime (T_{max}) heat waves identified in (14). A comparison of this index with daily T_{max} at the Portland International Airport reveals the positive correlation (Figure 4) for the bulk of the distribution of geopotential heights.

We estimate the "probable extreme" Portland temperature that would be associated with a given value of the GHI (Figure 4) by binning geopotential height data and determining the highest T_{max} observed for each bin in the historical period (1948-2020; excluding the 2021 event) (Methods). The linear regression curve of these upper-quantile values of temperature with respect to the GHI is plotted in the dark gray line of Fig, 4. This regression analysis demonstrates that the extreme value of the GHI in June 2021 provided a physical line of evidence for the risk of occurrence of the most extreme heat wave event in Portland in the modern climate. The 95% confidence intervals for in-sample uncertainty (shaded grey band) and out-of-sample/prediction uncertainty (dashed lines) are also shown. Given our estimated range of the probability of the 2021 event from the GPD analysis (0.01% - 2%) it is perhaps unsurprising that the most extreme day of the heat wave June 28th (46.7°C) falls above our 95% prediction confidence interval.

Splitting the period of record from 1948-2020 into two distinct time periods 1948-1983 and 1984-2020 (Methods) we find that the central value of the GHI and daily T_{max} both shift to higher values consistent with estimations of current impacts of anthropogenic climate change. Importantly, however, no significant change in the slope of the linear relationship between GHI and Portland T_{max} is found from the early period to the late period of the historical record (Figure 4). This indicates that the GHI has comparable predictive power for Portland daytime T_{max} currently as it did before appreciable global warming occurred. This line of evidence indicates that the Portland heat wave was consistent with the historical relationship between atmospheric circulation and probable extreme temperatures and was primarily a result of record-breaking anomalies in the geopotential heights. The critical importance of anomalous atmospheric circulation for the extremeness of this event has been documented in more detail in (*40*)

The above evidence of a clear role for atmospheric dynamics in the Portland heat wave motivates a third line of statistical analysis based on stochastic theory. A stochastically generated

skew (SGS) distribution has been developed to explain the full PDF of many atmospheric quantities, and is a natural consequence of the quadratic, advective nonlinearities that dominate mid-latitude dynamics (*26*, *34*). In the SGS distribution, skewness and heavy (power-law) tails are inextricably linked by the dynamics of a multiplicative noise stochastic process. If one applies the SGS approach to all daily T_{max} for Portland for June 15th to July 15th, the return period of 116°F in Portland is 254 years (Methods), qualitatively in line with the GPD central estimate of 337 years(*41*). The SGS distribution has heavy (power-law) tails for parameters where the skewness is non-zero. Specifically, both tails of the SGS converge to the GPD with positive shape parameters for large extremes (*26*), providing further support for the GPD approach as a more appropriate estimator for these positively skewed regions.

Despite the observed historical and projected future increase in hot extremes across much of the western US, the PNW shows no significant increase in the frequency of T_{max} heat waves in the modern observed record (*9*, *10*, *42*). Additionally, there is little evidence for historical magnification of the intensity of heat waves (*42*) or heat stress days (*43*) over recent decades in the PNW. In general terms, small increases to the mean and variance of the distribution of T_{max} have been shown to significantly increase the probability of temperature extremes (*13*), but evaluation of the observed impact of changes to skewness remains uncertain and regionally variable. Nonetheless there is some indication that projected declines in the skewness of the T_{max} could lead to less intense warm summer anomalies in the PNW (*44*), while in contrast, regional and global climate models suggest that hot extremes have increased in likelihood in the historical period across much of the interior western US (*45*) and will continue to increase as mean global temperature rises (*46*, *47*).

For much of the rest of the US, the negative skewness of daily T_{max} has been cited as a factor that allows for more effective detection of the influence of climate change on the frequency of heat waves as mean temperatures warm (*16*). Conversely, for the PNW and coast regions, the positive skewness of daily T_{max} would make detection of a climate change signal on heat wave frequency more difficult. Whether climate change may affect atmospheric dynamics itself and thereby alter heat wave risks, for instance via resonant amplification in 500 hPa height anomalies (*48–50*) is an open question. However, given that our analysis points to an extreme circulation anomaly as the primary driver of this event, further investigation of this connection is warranted.

4. Conclusions

The June PNW heat wave of 2021 was rare by all accounts. However, multiple lines of evidence indicate that the possibility of an event of this magnitude could have been foreseen using only data from prior years. The positive skewness of daily T_{max} in the PNW informs that large excursions in temperature are rare, but possible in this region. This positive skewness has been seen in the observational record of coastal regions, but the maritime influence extends much farther inland in the PNW, which primes the region for "surprise" extreme temperature events. This can be contrasted with regions such as the interior southwest US, where the strong negative skewness of the probability distribution of daily T_{max} reflects a smaller probability of extreme heat wave "surprises".

The regional 500 hPa height anomalies were unprecedented in magnitude during late June 2021. However, the circulation regime over the PNW region showed the same spatial pattern as other historical heat waves. Given the strong relationship between the height anomalies and maximum surface temperatures, one could have anticipated a heat wave of record-breaking magnitude if one could have foreseen the heights. Indeed, sub-seasonal numerical weather prediction models did foresee the late June 2021 circulation pattern(*40*), and this factor was cited by National Weather Service forecasters in the days leading up to the event (*51*).

Though the positive skewness of the daily T_{max} is limited to coastal regions of the western US and the extended PNW region, the large population of those regions gives cause for further consideration of skewness in the estimation of extreme heat risk. A similar, though less extreme, heat wave in 2006 in coastal central California led to a disproportionate number of hospitalizations (*52*) and is indicative of the risk of large and outwardly surprising temperature anomalies in these regions. If a record-breaking event as extreme as the 2021 PNW heat wave is considered all but "impossible" based on a particular statistical inference, then there is diminished potential for effective planning for such an event. Here we have demonstrated that an alternative statistical analysis of the historical record could have forewarned of the possibility for an event akin to the 2021 PNW heat wave based solely on historical observations. A statistical approach that appropriately captures the underlying dynamics–as reflected in the skewness and potentially heavy-tailed nature of the distribution–can support a more proactive approach to risk management for future extremes.

References and Notes

1. J. Silberner, Heat wave causes hundreds of deaths and hospitalisations in Pacific north west. *BMJ*, n1696 (2021).

2. A. Vaughan, The heat is on out west. *New Scientist*. **250**, 10–10 (2021).

3. S. Y. Philip, S. F. Kew, G. J. van Oldenborgh, W. Yang, G. A. Vecchi, F. S. Anslow, S. Li, S. I. Seneviratne, L. N. Luu, J. Arrighi, R. Singh, van Aalst, M. Hauser, D. L. Schumacher, C. P. Marghidan, K. L. Ebi, R. Bonnet, R. Vautard, J. Tradowsky, D. Coumou, F. Lehner, C. Rodell, R. Stull, R. Howard, N. Gillett, F. E. L. Otto, Rapid attribution analysis of the extraordinary heatwave on the Pacific Coast of the US and Canada June 2021., 37.

4. M. J. Menne, I. Durre, B. Korzeniewski, S. McNeill, K. Thomas, X. Yin, S. Anthony, R. Ray, R. S. Vose, B. E. Gleason, T. G. Houston, Global Historical Climatology Network - Daily (GHCN-Daily), Version 3 (2012), , doi:10.7289/V5D21VHZ.

5. An Excessive Heat Warning was issued by the NOAA National Weather Service Portland OR forecast office on Wednesday 23 June 2021 at 3:11 PM PDT that noted "UNPRECEDENTED HEAT EXPECTED THIS WEEKEND INTO NEXT WEEK". Retrieved from https://mesonet.agron.iastate.edu/wx/afos/p.php?pil=NPWPQR&e=202106232211 on 3 March 2022.

6. Evan Bush, Hal Bernton, "Jaw-dropping" forecast is warning sign of climate change's future impact in Washington, scientists say. *Seattle Times* (2021), (available at https://www.seattletimes.com/seattle-news/jaw-dropping-forecast-is-warning-sign-of-climate-changes-future-impact-in-washington-scientists-say/).

7. K. Guirguis, A. Gershunov, D. R. Cayan, D. W. Pierce, Heat wave probability in the changing climate of the Southwest US. *Clim Dyn*. **50**, 3853–3864 (2018).

8. A. Gershunov, K. Guirguis, California heat waves in the present and future. *Geophysical Research Letters*. **39** (2012), doi:10.1029/2012GL052979.

9. E. M. Oswald, An Analysis of the Prevalence of Heat Waves in the United States between 1948 and 2015. *Journal of Applied Meteorology and Climatology*. **57**, 1535–1549 (2018).

10. K. A. Bumbaco, K. D. Dello, N. A. Bond, History of Pacific Northwest Heat Waves: Synoptic Pattern and Trends. *Journal of Applied Meteorology and Climatology*. **52**, 1618–1631 (2013).

11. G. S. Mauger, J. S. Casola, H. A. Morgan, R. L. Strauch, B. Jones, B. Curry, T. M. Busch Isaksen, L. Whitley Binder, M. B. Krosby, A. K. Snover, "State of Knowledge: Climate Change in Puget Sound" (Climate Impacts Group, UW Seattle, 2015), (available at https://cig.uw.edu/resources/special-reports/ps-sok/).

12. P. Stott, How climate change affects extreme weather events. *Science*. **352**, 1517–1518 (2016).

13. L. O. Mearns, R. W. Katz, S. H. Schneider, Extreme High-Temperature Events: Changes in their probabilities with Changes in Mean Temperature. *Journal of Applied Meteorology and Climatology*. **23**, 1601–1613 (1984).

14. M. L. Weitzman, On Modeling and Interpreting the Economics of Catastrophic Climate Change. *Review of Economics and Statistics*. **91**, 1–19 (2009).

15. M. L. Stein, Should annual maximum temperatures follow a generalized extreme value distribution? *Biometrika*. **104**, 1–16 (2017).

16. P. C. Loikith, J. D. Neelin, Short-tailed temperature distributions over North America and implications for future changes in extremes. *Geophysical Research Letters*. **42**, 8577–8585 (2015).

17. M. J. Menne, I. Durre, R. S. Vose, B. E. Gleason, T. G. Houston, An Overview of the Global Historical Climatology Network-Daily Database. *Journal of Atmospheric and Oceanic Technology*. **29**, 897–910 (2012).

18. D. Zwillinger, S. Kokoska, *CRC standard probability and statistics tables and formulae* (Chapman & Hall/CRC, Boca Raton, 2000).

19. J. R. M. Hosking, J. R. Wallis, E. F. Wood, Estimation of the Generalized Extreme-Value Distribution by the Method of Probability-Weighted Moments. *Technometrics*. **27**, 251–261 (1985).

20. P. Virtanen, R. Gommers, T. E. Oliphant, M. Haberland, T. Reddy, D. Cournapeau, E. Burovski, P. Peterson, W. Weckesser, J. Bright, S. J. van der Walt, M. Brett, J. Wilson, K. J. Millman, N. Mayorov, A. R. J. Nelson, E. Jones, R. Kern, E. Larson, C. J. Carey, İ. Polat, Y. Feng, E. W. Moore, J. VanderPlas, D. Laxalde, J. Perktold, R. Cimrman, I. Henriksen, E. A. Quintero, C. R. Harris, A. M. Archibald, A. H. Ribeiro, F. Pedregosa, P. van Mulbregt, SciPy 1.0 Contributors, SciPy 1.0: Fundamental Algorithms for Scientific Computing in Python. *Nature Methods*. **17**, 261–272 (2020).

21. E. Castillo, A. S. Hadi, Fitting the Generalized Pareto Distribution to Data. *Journal of the American Statistical Association*. **92**, 1609–1620 (1997).

22. J. R. M. Hosking, J. R. Wallis, Parameter and Quantile Estimation for the Generalized Pareto Distribution. *Technometrics*. **29**, 339–349 (1987).

23. S. Coles, "Threshold Models" in *An Introduction to Statistical Modeling of Extreme Values*, S. Coles, Ed. (Springer London, London, 2001; https://doi.org/10.1007/978-1-4471-3675-0_4), pp. 74–91.

24. S. Saeed Far, A. K. Abd. Wahab, “Evaluation of Peaks-Over-Threshold Method” (preprint, Surface/Numerical Models/China Sea/Surface Waves, 2016), , doi:10.5194/os-2016-47.

25. A. G. Barnston, B. Lyon, E. D. Coffel, R. M. Horton, Daily Autocorrelation and Mean Temperature/Moisture Rise as Determining Factors for Future Heat-Wave Patterns in the United States. *Journal of Applied Meteorology and Climatology*. **59**, 1735–1754 (2020).

26. P. D. Sardeshmukh, G. P. Compo, C. Penland, Need for Caution in Interpreting Extreme Weather Statistics. *Journal of Climate*. **28**, 9166–9187 (2015).

27. M. Holický, *Introduction to Probability and Statistics for Engineers* (Springer Berlin Heidelberg, Berlin, Heidelberg, 2013; http://link.springer.com/10.1007/978-3-642-38300-7).

28. P. Dragicevic, "Fair Statistical Communication in HCI" in *Modern Statistical Methods for HCI*, J. Robertson, M. Kaptein, Eds. (Springer International Publishing, Cham, 2016; http://link.springer.com/10.1007/978-3-319-26633-6_13), *Human–Computer Interaction Series*, pp. 291–330.

29. M. Waskom, O. Botvinnik, D. O'Kane, P. Hobson, S. Lukauskas, D. C. Gemperline, T. Augspurger, Y. Halchenko, J. B. Cole, J. Warmenhoven, J. de Ruiter, C. Pye, S. Hoyer, J. Vanderplas, S. Villalba, G. Kunter, E. Quintero, P. Bachant, M. Martin, K. Meyer, A. Miles, Y. Ram, T. Yarkoni, M. L. Williams, C. Evans, C. Fitzgerald, Brian, C. Fonnesbeck, A. Lee, A. Qalieh, mwaskom/seaborn: v0.8.1 (September 2017) (2017), , doi:10.5281/zenodo.883859.

30. M. Lefebvre, Ed., "Simple Linear Regression" in *Applied Probability and Statistics* (Springer New York, New York, NY, 2006; https://doi.org/10.1007/0-387-28505-9_7), pp. 307–338.

31. T. W. Ruff, J. D. Neelin, Long tails in regional surface temperature probability distributions with implications for extremes under global warming. *Geophysical Research Letters*. **39** (2012), doi:10.1029/2011GL050610.

32. R. E. S. Clemesha, K. Guirguis, A. Gershunov, I. J. Small, A. Tardy, California heat waves: their spatial evolution, variation, and coastal modulation by low clouds. *Clim Dyn*. **50**, 4285–4301 (2018).

33. P. C. Loikith, J. D. Neelin, J. Meyerson, J. S. Hunter, Short Warm-Side Temperature Distribution Tails Drive Hot Spots of Warm Temperature Extreme Increases under Near-Future Warming. *Journal of Climate*. **31**, 9469–9487 (2018).

34. P. D. Sardeshmukh, P. Sura, Reconciling Non-Gaussian Climate Statistics with Linear Dynamics. *Journal of Climate*. **22**, 1193–1207 (2009).

35. A. F. Jenkinson, The frequency distribution of the annual maximum (or minimum) values of meteorological elements. *Q.J Royal Met. Soc.* **81**, 158–171 (1955).

36. S. Philip, S. Kew, G. J. van Oldenborgh, F. Otto, R. Vautard, K. van der Wiel, A. King, F. Lott, J. Arrighi, R. Singh, M. van Aalst, A protocol for probabilistic extreme event attribution analyses. *Advances in Statistical Climatology, Meteorology and Oceanography*. **6**, 177–203 (2020).

37. V. V. Kharin, F. W. Zwiers, Estimating Extremes in Transient Climate Change Simulations. *Journal of Climate*. **18**, 1156–1173 (2005).

38. J. Pickands, Statistical Inference Using Extreme Order Statistics. *The Annals of Statistics*. **3**, 119–131 (1975).

39. A. Tancredi, C. Anderson, A. O'Hagan, Accounting for threshold uncertainty in extreme value estimation. *Extremes*. **9**, 87–106 (2006).

40. H. Lin, R. Mo, F. Vitart, *Geophysical Research Letters*, in press, doi:10.1029/2021GL097036.

41. C. A. Smith, G. P. Compo, D. K. Hooper, Web-Based Reanalysis Intercomparison Tools (WRIT) for Analysis and Comparison of Reanalyses and Other Datasets. *Bulletin of the American Meteorological Society*. **95**, 1671–1678 (2014).

42. S. E. Perkins-Kirkpatrick, S. C. Lewis, Increasing trends in regional heatwaves. *Nat Commun*. **11**, 3357 (2020).

43. K. Dahl, R. Licker, J. T. Abatzoglou, J. Declet-Barreto, Increased frequency of and population exposure to extreme heat index days in the United States during the 21st century. *Environ. Res. Commun.* **1**, 075002 (2019).

44. T. Tamarin-Brodsky, K. Hodges, B. J. Hoskins, T. G. Shepherd, Changes in Northern Hemisphere temperature variability shaped by regional warming patterns. *Nat. Geosci.* **13**, 414–421 (2020).

45. IPCC, "Climate Change 2021: The Physical Science Basis. Contribution of Working Group I to the Sixth Assessment Report of the Intergovernmental Panel on Climate Change [Masson-Delmotte, V., P. Zhai, A. Pirani, S.L. Connors, C. Péan, S. Berger, N. Caud, Y. Chen, L. Goldfarb, M.I. Gomis, M. Huang, K. Leitzell, E. Lonnoy, J.B.R. Matthews, T.K. Maycock, T. Waterfield, O. Yelekçi, R. Yu, and B. Zhou (eds.)]" (Cambridge University Press, 2021).

46. R. T. Clark, S. J. Brown, J. M. Murphy, Modeling Northern Hemisphere Summer Heat Extreme Changes and Their Uncertainties Using a Physics Ensemble of Climate Sensitivity Experiments. *Journal of Climate*. **19**, 4418–4435 (2006).

47. K. E. Kunkel, X.-Z. Liang, J. Zhu, Regional Climate Model Projections and Uncertainties of U.S. Summer Heat Waves. *Journal of Climate*. **23**, 4447–4458 (2010).

48. G. A. Meehl, C. Tebaldi, More Intense, More Frequent, and Longer Lasting Heat Waves in the 21st Century. *Science* (2004), doi:10.1126/science.1098704.

49. K. Kornhuber, D. Coumou, E. Vogel, C. Lesk, J. F. Donges, J. Lehmann, R. M. Horton, Amplified Rossby waves enhance risk of concurrent heatwaves in major breadbasket regions. *Nat. Clim. Chang.* **10**, 48–53 (2020).

50. M. E. Mann, S. Rahmstorf, K. Kornhuber, B. A. Steinman, S. K. Miller, D. Coumou, Influence of anthropogenic climate change on planetary wave resonance and extreme weather events. *Scientific Reports*. **7**, 45242 (2017).

51. The forecast of very anomalous 500 hPa heights was noted in the 233 PM PDT Sun Jun 20 2021 Area Forecast Discussion by the Portland National Weather Service forecast office., (available at https://mesonet.agron.iastate.edu/wx/afos/p.php?pil=AFDPQR&e=202106202133).

52. K. Knowlton, -Ellman Miriam Rotkin, G. King, H. G. Margolis, D. Smith, G. Solomon, R. Trent, P. English, The 2006 California Heat Wave: Impacts on Hospitalizations and Emergency Department Visits. *Environmental Health Perspectives*. **117**, 61–67 (2009).

Acknowledgments: The authors acknowledge the contributions of Jon Eischeid for providing the geopotential height index, and Gil Compo and Nachiketa Acharya for informative discussions on methodology.

Funding: Provide complete funding information, including grant numbers, complete funding agency names, and recipient's initials. Each funding source should be listed in a separate paragraph.
National Oceanic and Atmospheric Administration Climate Program Office funding through CIRES Cooperative Agreement NA17OAR4320101 (JB, XQ)

National Oceanic and Atmospheric Administration Climate Program Office grant # (NB)

Author contributions: Each author's contribution(s) to the paper should be listed [we encourage you to follow the CRediT model]. Each CRediT role should have its own line, and there should not be any punctuation in the initials.

Conceptualization: NB, JJB, MPH, BL
Investigation: NB, JJB, MPH, XWQ, BL
Visualization: NB, JJB
Funding acquisition: BL, JJB, MPH
Writing – original draft: NB
Writing – review & editing: NB, JJB, MPH, XWQ, BL

Competing interests: Authors declare that they have no competing interests.

Data and materials availability: Data and code will be made available on the zenodo.com archive

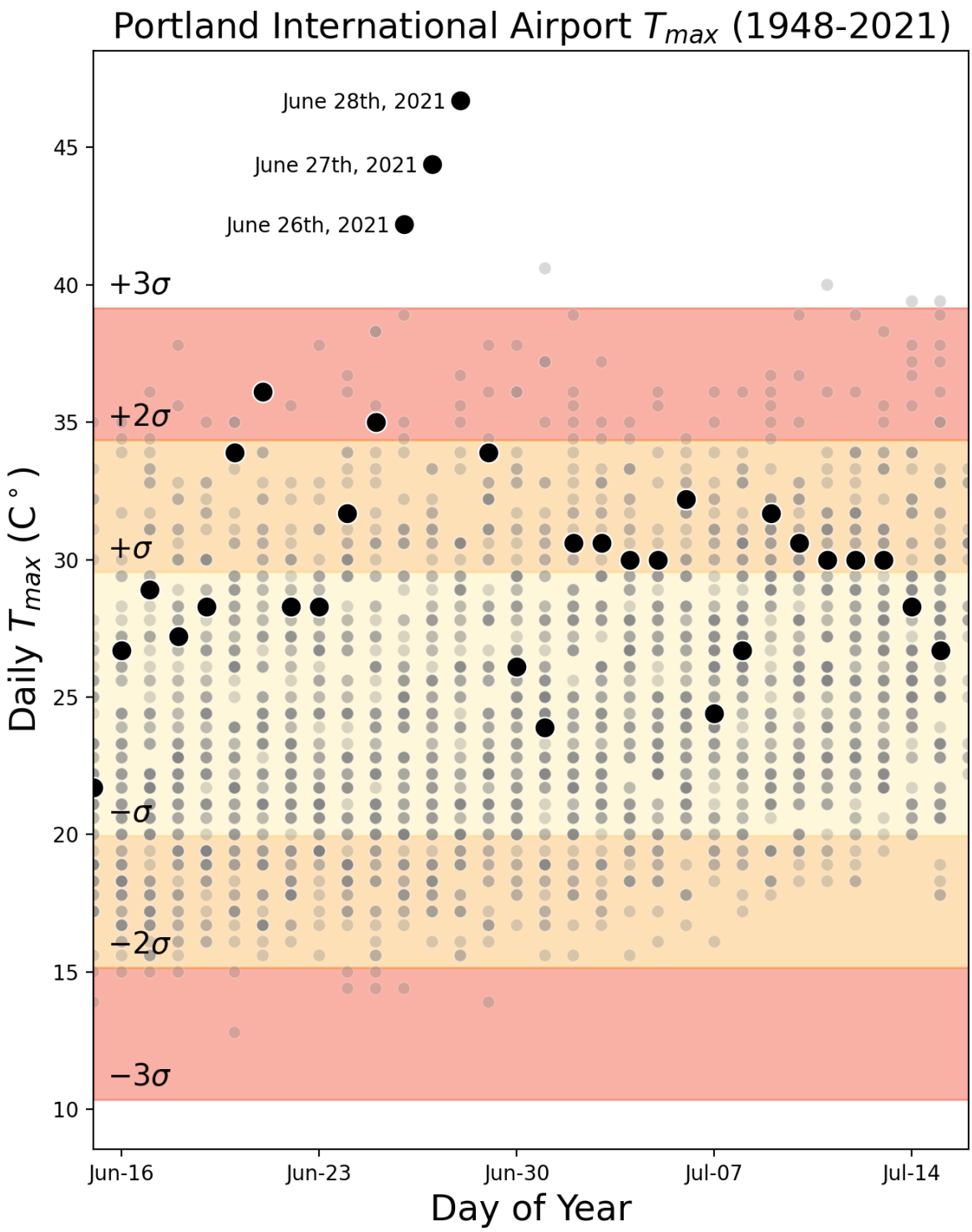

Fig. 1. Daily T_{max} from Portland International Airport (GHCN USW00024229) from 1948 to 2021 for June 15th to July 15th. The larger black points are all of the daily T_{max} values from 2021 with the points for the June PNW heat wave labelled. Transparent gray points are the daily T_{max} from 1948 to 2021. The yellow, orange, and red colored bands represent one, two and three standard deviations from the mean calculated from the daily T_{max} from the years 1948-2021.

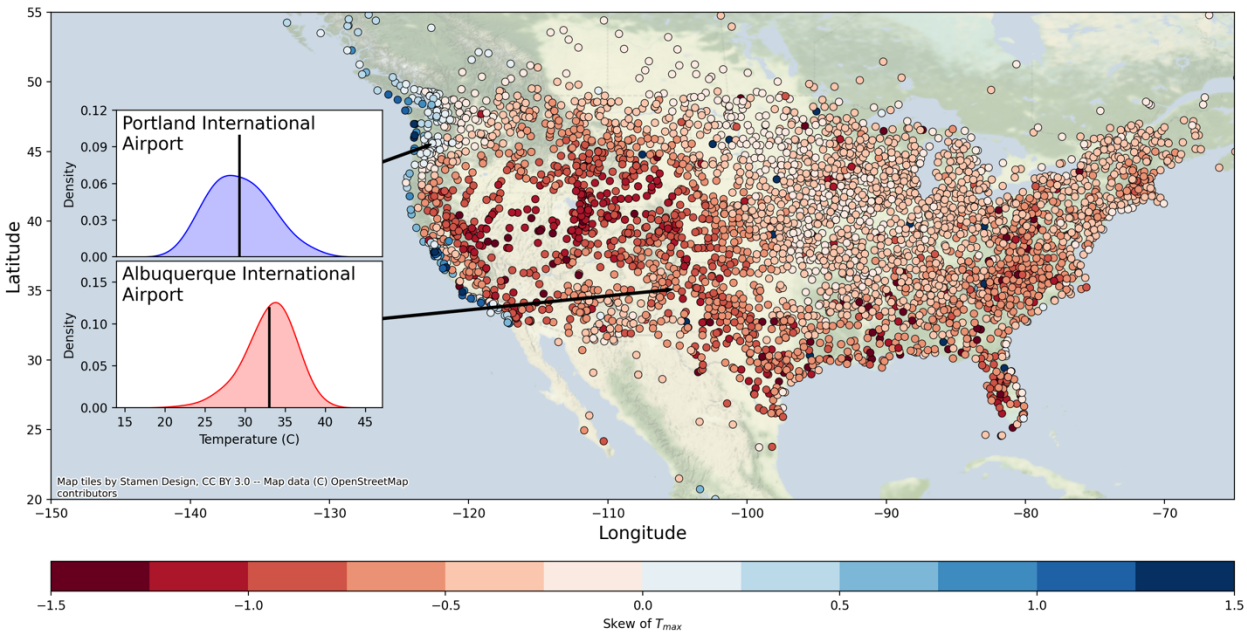

Fig. 2. Skewness of daily T_{max} probability distributions from 1948-2020 for June 15th to July 15th from GHCN stations that have sufficiently long and continuous records (Methods). Each point is a single GHCN station colored by the skewness of the daily T_{max} temperature distribution. The inset panels highlight two individual stations to demonstrate the

shape of distributions with both a positive (Portland International Airport, top inset panel) and negative (Albuquerque International Airport, bottom inset panel) T_{max} skew.

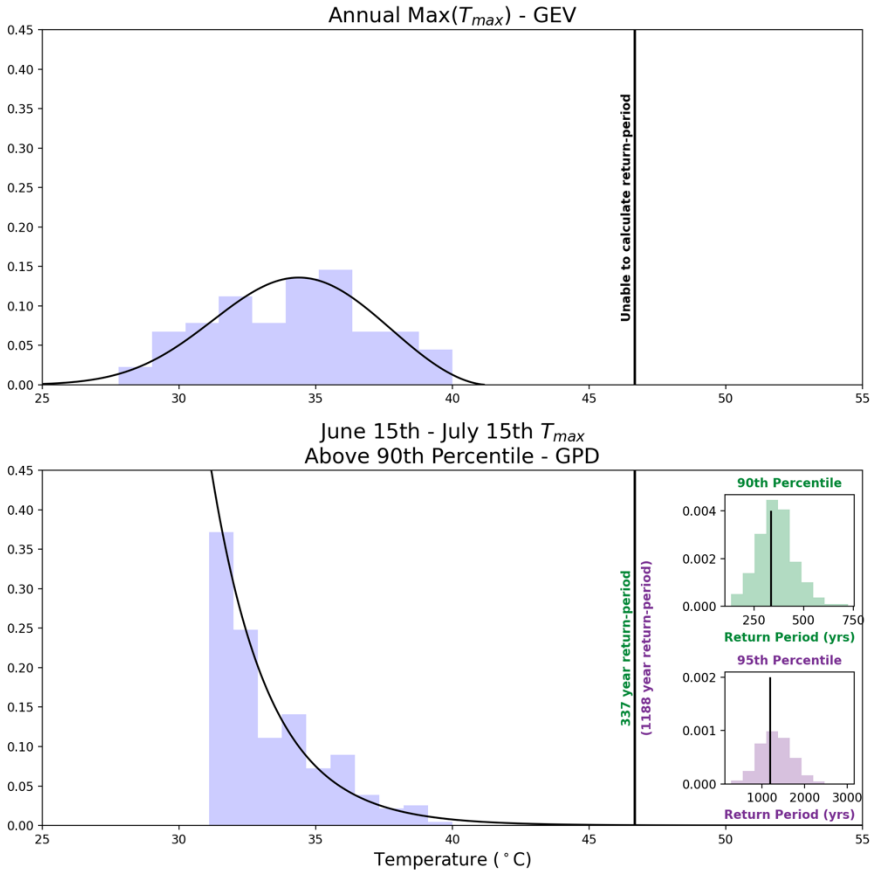

Fig. 3. Estimation of return period for PNW 2021 heat wave using GEV and GPD. Panel (a): Histogram of annual max T_{max} from Portland International Airport (GHCN USW00024229) from 1948 to 2020 (blue). The solid black curve shows the estimated GEV fit of the annual maximum T_{max} and the vertical line labelled "Unable to calculate return-period" reflects the temperature of the most extreme daily T_{max} of the June 2021 PNW heat wave (46.7°C). **Panel (b):** Histogram of daily T_{max} from Portland International Airport (GHCN USW00024229) from 1948 to 2020 for June 15th to July 15th (blue), only showing the data above the 90th percentile that was used for the GPD fit. The solid black curve shows the median estimated GPD fit of the annual maximum T_{max} and the same as in panel (a). The top right inset panel shows the histogram of the bootstrap-calculated return periods (10,000 samples) using a 90th percentile threshold (green) with the vertical black line showing the median estimated return period (337

years). The bottom right inset panel shows the same as the top inset panel using a 95th percentile threshold (purple) with a median estimated return period of (1,188 years).

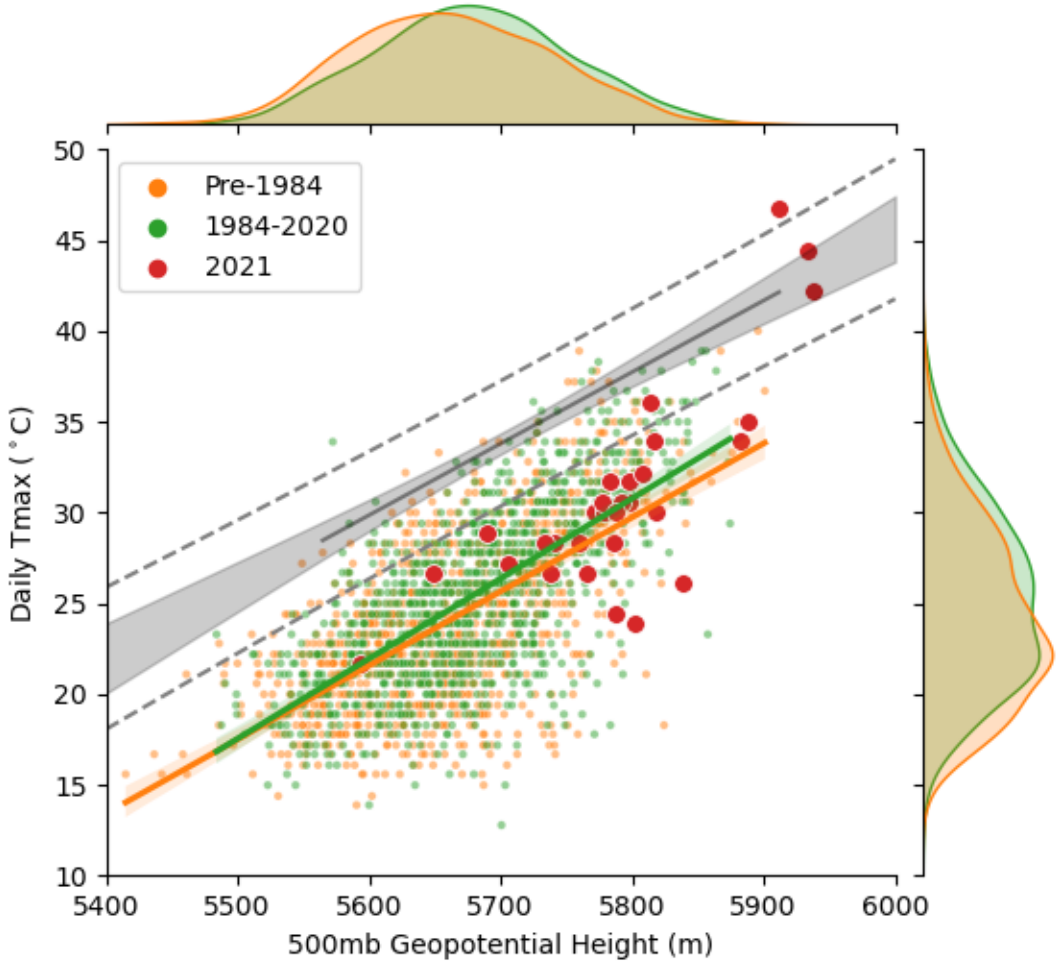

Fig 4. Daily observations of T_{max} and 500 hPa geopotential heights from Portland International Airport (GHCN USW00024229) from 1948 to 2021 for June 15th to July 15th. Observations are split into three groups by year: 1948-1983 (orange), 1984-2020 (green) and 2021 (red). Points represent daily observations for each group and solid colored lines show the linear regression for the entire population of each group with shaded 95% confidence intervals about the regression line. Non-parametric kernel density estimations of daily 500 hPa geopotential heights and daily T_{max} are plotted on the top and right axes respectively. The dark gray line shows the linear regression of the binned maximum T_{max} (Methods) with shaded 95%

confidence intervals for the regression line and dashed lines demonstrating the 95% out-of-sample confidence interval of the regression.